

100 Gb/s all-optical clock recovery based on a monolithic dual-mode DBR laser

Biwei Pan (潘碧玮)¹, Liqiang Yu (余力强)¹, Lu Guo (郭露)¹, Limeng Zhang (张莉萌)¹,
Dan Lu (陆丹)¹, Xin Chen (陈新)², Yue Wu (武岳)², Caiyun Lou (娄采云)²,
and Lingjuan Zhao (赵玲娟)^{1,*}

¹Key Laboratory of Semiconductor Materials Science, Institute of Semiconductors, Chinese Academy of Science, Beijing 100083, China

²Tsinghua National Laboratory for Information Science and Technology, State Key Laboratory of Integrated Optoelectronics, Department of Electronic Engineering, Tsinghua University, Beijing 100084, China

*Corresponding author: ljzhao@semi.ac.cn

Received August 16, 2015; accepted January 8, 2016; posted online February 26, 2016

We experimentally demonstrate all-optical clock recovery for 100 Gb/s return-to-zero on-off keying signals based on a monolithic dual-mode distributed Bragg reflector (DBR) laser, which can realize both mode spacing and wavelength tuning. By using a coherent injection locking scheme, a 100 GHz optical clock can be recovered with a timing jitter of 530 fs, which is derived by an optical sampling oscilloscope from both the phase noise and the power fluctuation. Furthermore, for degraded injection signals with an optical signal-to-noise ratio as low as 4.1 dB and a 25 km long distance transmission, good-quality optical clocks are all successfully recovered.

OCIS codes: 070.6020, 140.3520.

doi: 10.3788/COL201614.030604.

All-optical clock recovery (AOCR) is regarded as a key technique to construct high-speed all-optical networks with enhanced transparency and flexibility. It is an indispensable component for realizing all-optical 3R (retiming, reshaping, and reamplification) regeneration^[1,2], optical time-division demultiplexing^[3], optical sampling, and modulation format conversion^[4]. Several schemes have been demonstrated for AOCR, such as passive spectra filters^[5], optoelectronic oscillators^[6], mode-locked lasers^[7], Fabry-Perot lasers^[8-10], and dual-mode lasers^[11,12]. Among those schemes, monolithic dual-mode lasers provide an integrated solution for AOCR, and have been the subject of intense investigation due to their advantages in size and power consumption and their wide tuning range.

When the dual-mode laser is used for AOCR, there are two types of injection locking approaches^[13]. One is incoherent injection locking, which uses carrier-modulated sidebands induced by the injection optical signal to lock the two lasing modes of the device. This scheme is wavelength and polarization insensitive, but the speed is greatly limited by the carrier lifetime and needs a high injection power. Another is coherent injection locking, which uses the two carrier modes to align and lock the two lasing modes of the laser. Optical injection locking then takes place simply by stimulated emission. This method needs a lower injection power and does not have a speed limitation, which is more suitable for future high-speed optical communication systems. However, coherent injection locking is wavelength sensitive. Therefore, the design and fabrication of a wavelength-tunable dual-mode laser is essential in practical applications.

In our previous work^[14], a monolithic dual-mode distributed Bragg reflector (DBR) laser was reported as

achieving both mode spacing and wavelength tuning. It is a four-section device integrated by a quantum well intermixing (QWI) technique. Due to the simple fabrication process, high-frequency mode separation, and wavelength tuning characteristics, this device is an attractive candidate for high-speed AOCR.

In this Letter, we report our experimental results on AOCR for a 100 Gb/s return-to-zero (RZ) on-off keying (OOK) signal using a monolithic dual-mode DBR laser with a pigtailed fiber in a normal butterfly package. Based on the coherent injection locking scheme, a 100 GHz optical clock is recovered with a timing jitter of 530 fs derived from both the phase noise and power fluctuation by an optical sampling oscilloscope (OSO) with a bandwidth of 500 GHz (EXFO-PSO-102C). Furthermore, the robustness of the AOCR on the properties of the injected signal is investigated through studying the dependence of the timing jitter of the recovery clock on the optical signal-to-noise ratio (OSNR) and long-distance transmission. The experiments show the dual-mode DBR's ability to extract a good-quality optical clock from degraded signals.

Figure 1 shows the schematic diagram of the proposed DBR-based AOCR. The transmitter used to generate the 100 Gb/s RZ-OOK signal is shown in the light brown box in Fig. 1. It is based on a 25 GHz, 2 ps optical pulse source, which is modulated by a LiNbO₃ intensity modulator with a 25 Gb/s 2³¹-1 pseudorandom bit sequence generated from a bit error rate (BER) tester (Agilent N4901B). A fiber-based, passive polarization-maintaining 1 × 4 multiplexer then multiplexes the optical signal to 100 Gb/s. The modulated signal first passes through an optical bandpass filter (OBPF, 5 nm) to eliminate extra noise, and then is injected into the pigtailed laser through an

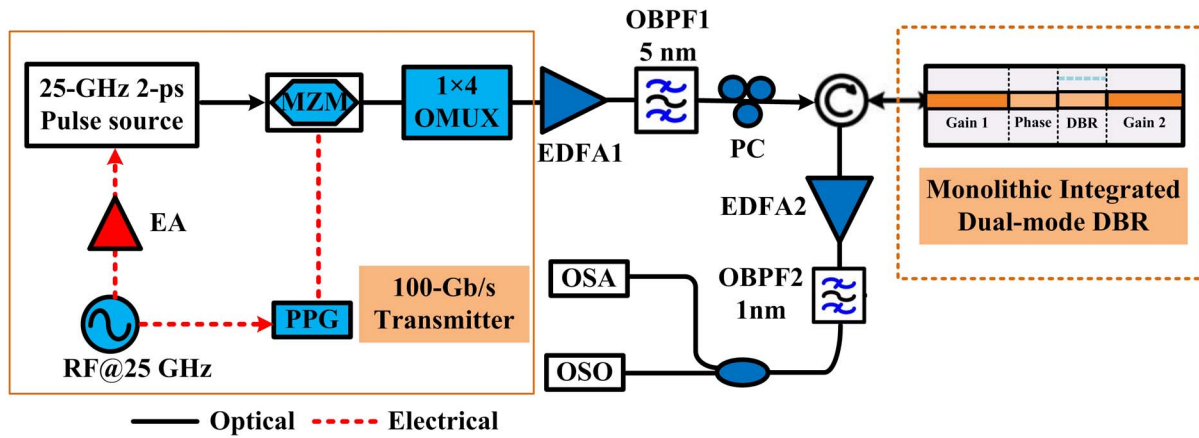


Fig. 1. Schematic diagram of the proposed DBR-based AOCR. MZM, Mach-Zehnder modulator; EA, electronic amplifier; OMUX, passive polarization maintaining 1×4 optical multiplexer.

optical circulator (OC). A polarization controller (PC) is used before port 1 of the OC to control the polarization alignment of the injection signal with the waveguide. The output of the laser is amplified by an erbium-doped fiber amplifier (EDFA) and passed through another OBPF (1 nm) to eliminate unwanted amplified spontaneous emission (ASE) noise. At last, the recovered clock signal is observed by an OSO and an optical spectrum analyzer (OSA).

As shown in the dashed box in Fig. 1, the key device of our scheme is the dual-mode DBR laser. It is a monolithic four-section laser consisting of a front gain section (gain 1), a phase section, a DBR section, and a rear gain section (gain 2) with lengths of 200, 100, 150, and 200 μm , respectively. Different laser sections are integrated by the simple QWI technology. The first three laser sections construct a conventional DBR laser, which works in the single-mode state due to the mode selection of the DBR grating. The rear gain section function as a resonant reflector modulating the end reflectivity of the lasing modes. By utilizing the proper bias current in this section, two modes with comparable threshold gains would lase simultaneously. Detailed information on the fabrication and performance of this device is presented in Ref. [12]. In the experiment, the DBR laser is packaged with a fiber pigtail from the uncoated facet of the front gain section, and the temperature is controlled at 25°C through a thermoelectric cooler.

Firstly, the free-running state of the DBR laser is investigated. The threshold current of the device is 35 mA. When the current of the front gain section (I_{g1}) is 70 mA with unbiased other sections, the laser works in the single-mode state and the output power is 3 mW. Dual-mode lasing can be achieved when the bias currents of the phase (I_P) and rear gain (I_{g2}) sections are appropriately adjusted. Figure 2(a) shows the typical optical spectrum of the dual-mode DBR, where (I_{g1} , I_P , I_{DBR} , and I_{g2}) are set as (70, 0, 20, and 8.2 mA). The mode spacing is about 0.8 nm, corresponding to a beating frequency

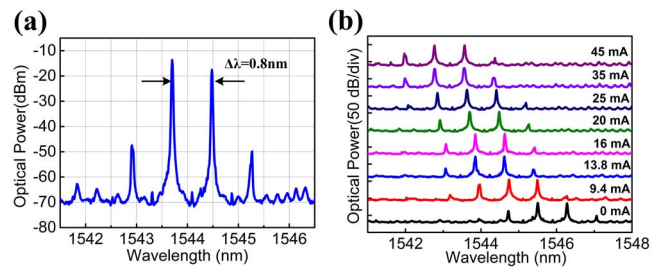


Fig. 2. (a) Typical free-running optical spectrum of the dual-mode DBR laser. (b) Optical spectra of the device under different DBR currents.

of 100 GHz. The two side modes with the same mode separation as the two main peaks are induced by four-wave mixing, which indicates a strong phase correlation between the two main modes.

Then, we investigate the wavelength tuning performance of the device. As shown in Fig. 2(b), with the increase of I_{DBR} , the wavelength of the two main modes will blue shift simultaneously with a nearly unchanged mode separation. The wavelengths of the device can be tuned in a 2.7 nm range by tuning I_{DBR} . This wavelength-tuning characteristic is very useful when aligning the wavelengths with the data signal in the coherent injection locking approach.

After that, we characterize the performance of the device for the AOCR. Figures 3(a) and 3(c) show the optical spectrum and eye diagram of the multiplexed 100 Gb/s RZ-OOK signal, where the OSNR is 22 dB. The measured time jitter of this signal is 163 fs, which comes from the jitter of the microwave source and multiple current sources of the devices, and the noise in the electronic amplifiers, modulators, and optical fibers. It also contains a 50 fs jitter of the OSO itself. The central wavelength of the signal is set at 1544 nm through OBPF1, which is almost the same as a free-running DBR. The injection power is set at 5 dBm and is measured before port 1 of the circulator.

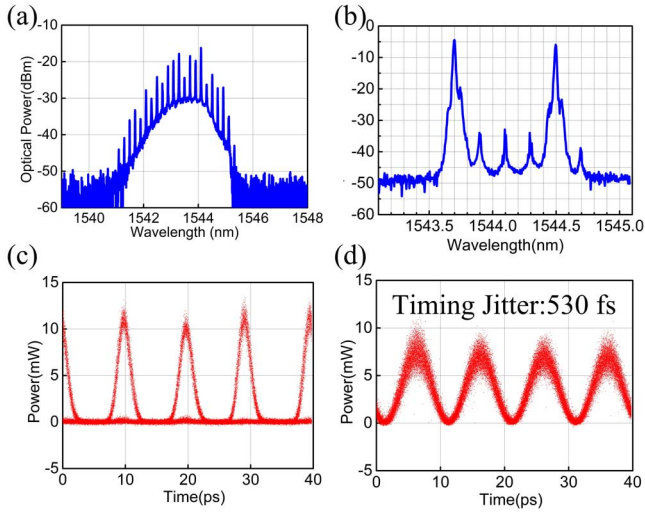


Fig. 3. (a) Optical spectrum of the 100 Gb/s RZ-OOK signal and (b) injection-locked dual-mode DBR laser. (c) Eye diagram of the 100 Gb/s signal. (d) Time trace of the recovered 100 GHz optical clock.

By slight tuning the bias current of the DBR section, the signal carrier is aligned to one mode of the DBR laser while one of the sidebands is aligned to another mode of the device. The two lasing modes would then be injection locked and phase synchronized to the injection signal. The injection-locked optical spectrum is shown in Fig. 3(b). The pedestals in the spectrum are due to the reflection from the uncoated facet of both the device and the fiber. There are also some modes on the pedestal with a mode spacing of 25 GHz, such as an optical clock of the 25 Gbit component resulting from imperfect multiplexing. Finally, a synchronized clock signal is obtained from the beating of the two locked modes. The recovered clock is shown in Fig. 3(d). The timing jitter of this signal is 530 fs, which is derived from both the phase noise and power fluctuation by the OSO. This jitter contains a 163 fs jitter floor transferred from the input signal through optical injection locking process. Such a timing jitter would typically result in a BER attributable to a clock jitter of less than 10^{12} ^[15], assuming a reasonable clock source for signal regeneration.

In order to investigate the robustness of the AOOCR for degraded injected signals, two experiments are carried out. Firstly, the OSNR of the injection signal is adjusted by adding a power-variable ASE noise source together with the signal source. By tuning the power ratio of the ASE source, the OSNR of the injected pulse train can be changed from 22 to 4.1 dB. The injection power is kept as 5 dBm in the measurement. Figures 4(a) and 4(b) show the eye diagram of the injected signal with the 4.1 dB OSNR and the recovered clock trace, respectively. The time jitter of the recovered clock increases to 834 fs at a 4.1 dB OSNR. When the OSNR drops below 4 dB, stable optical clock cannot be obtained because there is too much noise in the input signal. The measured timing jitter as a function of the OSNR is plotted in Fig. 4(c).

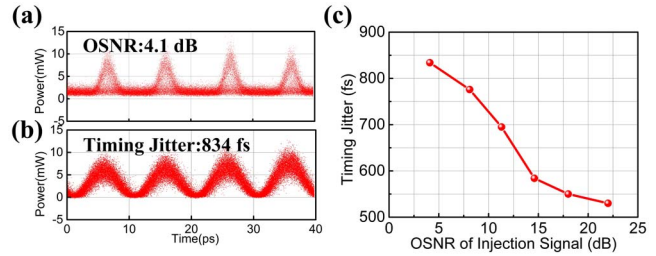


Fig. 4. (a) Degraded 100 Gb/s injection signal with 4.1 dB OSNR. (b) Time trace of the recovered optical clock. (c) The dependence of the timing jitter of the synchronized clock on the OSNR of the injected signal.

As can be seen, the DBR-based AOOCR is robust to OSNR degradations.

Secondly, the AOOCR for the signal transmitted with a 25 km single-mode fiber is investigated. For the signal after long-distance transmission, the time trace is degraded dramatically, mainly due to the chromatic dispersion. The eye diagram after transmission is shown in Fig. 5(a), which is so vague that one can hardly make out the OSNR. However, the chromatic dispersion will not degrade the signal in the frequency domain so much, and it will not weaken the clock component. As we can see, there is no obvious degradation shown in the optical spectra before [Fig. 3(a)] and after [Fig. 5(c)] transmission. Since the principle of the clock recovery using the dual-mode laser is optical injection locking fulfilled in the frequency domain, our scheme can realize clock extraction from a greatly chromatic dispersed signal after long-distance transmission. After injection locking with 5 dBm injection strength, clock recovery can be realized as the waveform shown in Fig. 5(b). A timing jitter of 760 fs is achieved. The injection-locked optical spectrum of the laser is also shown in Fig. 5(d).

In conclusion, we demonstrate AOOCR for 100 Gb/s RZ-OOK signals using a monolithic dual-mode DBR laser,

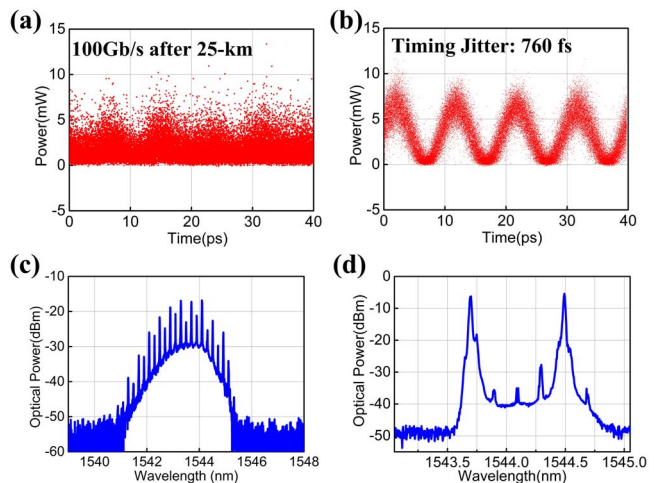


Fig. 5. (a) Eye diagrams and (b) optical spectrum of the 100 Gb/s signal after 25 km transmission. (b) Time trace of the recovered optical clock. (d) Injection-locked optical spectrum of the DBR laser.

which can realize both mode spacing and wavelength tuning. Based on the coherent injection approach, a 100 GHz optical clock is recovered with a timing jitter of 530 fs, which is derived from both the phase noise and power fluctuation by an OSO. Moreover, for degraded injection signals with an OSNR as low as 4.1 dB and a 25 km long-distance transmission, good-quality clock recoveries are experimentally realized, which indicates the robustness of the DBR-based AOCR on the property of injection signals. These results show the dual-mode DBR's potential application in compact and low-cost clock recovery for high-speed all-optical networks.

This work was supported by the National 973 Program of China (Nos. 2011CB301702 and 2011CB301703) and the National Natural Science Foundation of China (Nos. 61201103, 61335009, and 61321063).

References

1. X. Zhao, L. Wang, D. Lu, C. Lou, Y. Sun, L. Zhao, and W. Wang, in *Proceedings of Wireless and Optical Communications Conference*, 1 (2010).
2. Y. A. Leem, D. C. Kim, E. Sim, S.-B. Kim, H. Ko, K. H. Park, D.-Y. Yee, J. Oh, S. Lee, and M. Jeon, *IEEE J. Sel. Top. Quantum Electron.* **12**, 726 (2006).
3. Y. Ji, X. Jia, Y. Li, J. Wu, and J. Lin, *Chin. Opt. Lett.* **11**, 050602 (2013).
4. Q. Wang, L. Huo, Y. Xing, C. Lou, and B. Zhou, *IEEE Photon. Technol. Lett.* **25**, 2339 (2013).
5. M. Jinno, T. Matsumoto, and M. Koga, *IEEE Photon. Technol. Lett.* **2**, 203 (1990).
6. Q. Wang, L. Huo, Y. Xing, C. Lou, D. Wang, X. Chen, and B. Zhou, *Opt. Commun.* **320**, 22 (2014).
7. S. Arahira, S. Sasaki, K. Tachibana, and Y. Ogawa, *IEEE Photon. Technol. Lett.* **16**, 1558 (2004).
8. X. Tang, J. C. Cartledge, A. Shen, F. Van Dijk, and G.-H. Duan, *IEEE Photon. Technol. Lett.* **20**, 2051 (2008).
9. M. Costa e Silva, A. Lagrost, L. Bramerie, M. Gay, P. Besnard, M. Joindot, J. C. Simon, A. Shen, and G. H. Duan, in *Proceedings of the Conference Optical Fiber Communication, Collocated. National Fiber Optics Engineering Conference*, PDPC4 (2010).
10. J. Parra-Cetina, J. Luo, N. Calabretta, S. Latkowski, H. J. Dorren, and P. Landais, *J. Lightwave Technol.* **31**, 3127 (2013).
11. Y. Sun, J. Q. Pan, L. J. Zhao, W. Chen, W. Wang, L. Wang, X. Zhao, and C. Lou, *J. Lightwave Technol.* **28**, 2521 (2010).
12. L. Yu, Y. Li, J. Zang, D. Lu, B. Pan, and L. Zhao, *Chin. Opt. Lett.* **12**, 081402 (2014).
13. J. Qiu, C. Chen, L. Zhao, Y. Sun, D. Lu, C. Lou, and W. Wang, *Appl. Opt.* **51**, 2894 (2012).
14. L. Yu, D. Lu, L. Zhao, Y. Li, C. Ji, J. Pan, H. Zhu, and W. Wang, *IEEE Photon. Technol. Lett.* **25**, 576 (2013).
15. M. Jinno, *IEEE J. Quantum. Electron.* **30**, 2842 (1994).